Title

All-Inorganic Metal Halide Perovskite Nanocrystals: Opportunities and Challenges.

Journal

ACS central science, 4(6)

ISSN

2374-7943

Authors

Zhang, Qiao

Yin, Yadong

Publication Date

2018-06-01

DOI

10.1021/acscentsci.8b00201

Peer reviewed

ACS central science

Outlook

Cite This: ACS Cent. Sci. 2018, 4, 668–679

All-Inorganic Metal Halide Perovskite Nanocrystals: Opportunities and Challenges

Qiao Zhang[†] and Yadong Yin*[,‡]

[†]Institute of Functional Nano and Soft Materials (FUNSOM), Jiangsu Key Laboratory for Carbon-Based Functional Materials and Devices, Soochow University, 199 Ren'ai Road, Suzhou, Jiangsu 215123, People's Republic of China

[‡]Department of Chemistry, University of California, Riverside, Riverside, California 92521, United States

ABSTRACT: The past decade has witnessed the growing interest in metal halide perovskites as driven by their promising applications in diverse fields. The low intrinsic stability of the early developed organic versions has however hampered their widespread applications. Very recently, all-inorganic perovskite nanocrystals have emerged as a new class of materials that hold great promise for the practical applications in solar cells, photodetectors, light-emitting diodes, and lasers, among others. In this Outlook, we first discuss the recent developments in the preparation, properties, and applications of all-inorganic metal halide perovskite nanocrystals, with a particular focus on $CsPbX_3$, and then provide our view of current challenges and future directions in this emerging area. Our goal is to introduce the current status of this type of new materials to researchers from different areas and motivate them to explore all the potentials.

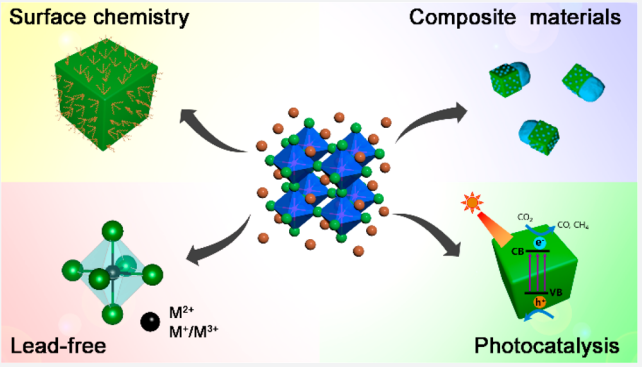

INTRODUCTION

Everything seems to be speeding up in the new century, especially in the field of scientific research. For example, researchers have spent more than 20 years to achieve a photoconversion efficiency (PCE) of over 20% for silicon-based (Si-based) photovoltaics.[1] In striking contrast, the PCE of solar cells based on metal halide perovskite (ABX_3, where A = organic group; B = Pb, Sn, Sb, etc.; X = Cl, Br, or I) has been rapidly promoted from ∼3.8% to over 22% within just several years.[2−5] In addition to solar cells, various applications have been demonstrated based on metal halide perovskite materials, such as light-emitting diodes (LEDs),[6,7] photodetectors,[8] lasers,[9,10] flexible electronics,[11] and so on. Many scalable manufacturing protocols have also been developed in a relatively short period to meet the demand of practical applications, along with more detailed characterizations of their physiochemical properties by state-of-the-art instruments. As a result, thousands of papers on these emerging materials have been published over the past several years.

Despite the great success of organic metal halide perovskite (OHP) materials, several problems remain to be resolved, including particularly their long-term stability under ambient condition. It has been discovered that they are sensitive to many factors, such as moisture, oxygen, light, and heat.[12] Although many methods have been proposed to solve the problem, the low intrinsic stability of organic metal halide perovskite materials originated from the organic groups has not been improved significantly. It is, therefore, not a surprising idea to replace the organic group with inorganic ions to produce all-inorganic metal halide perovskite (IHP) materials.[13]

Although many methods have been proposed to solve the problem, the low intrinsic stability of organic metal halide perovskite materials originated from the organic groups has not been improved significantly. It is, therefore, not a surprising idea to replace the organic group with inorganic ions to produce all-inorganic metal halide perovskite (IHP) materials.

In 2015, the Kovalenko group reported the first successful preparation of $CsPbX_3$ nanocrystals (NCs) using a hot-injection method.[14] Compared with the OHP materials, the $CsPbX_3$ materials possess several advantages, including a higher melting point (>500 °C), higher thermal stability, and higher stability against photobleaching, which make them more suitable candidates for optoelectronic applications.[15,16] The

Received: April 3, 2018
Published: May 29, 2018

DOI: 10.1021/acscentsci.8b00201
ACS Cent. Sci. 2018, 4, 668–679

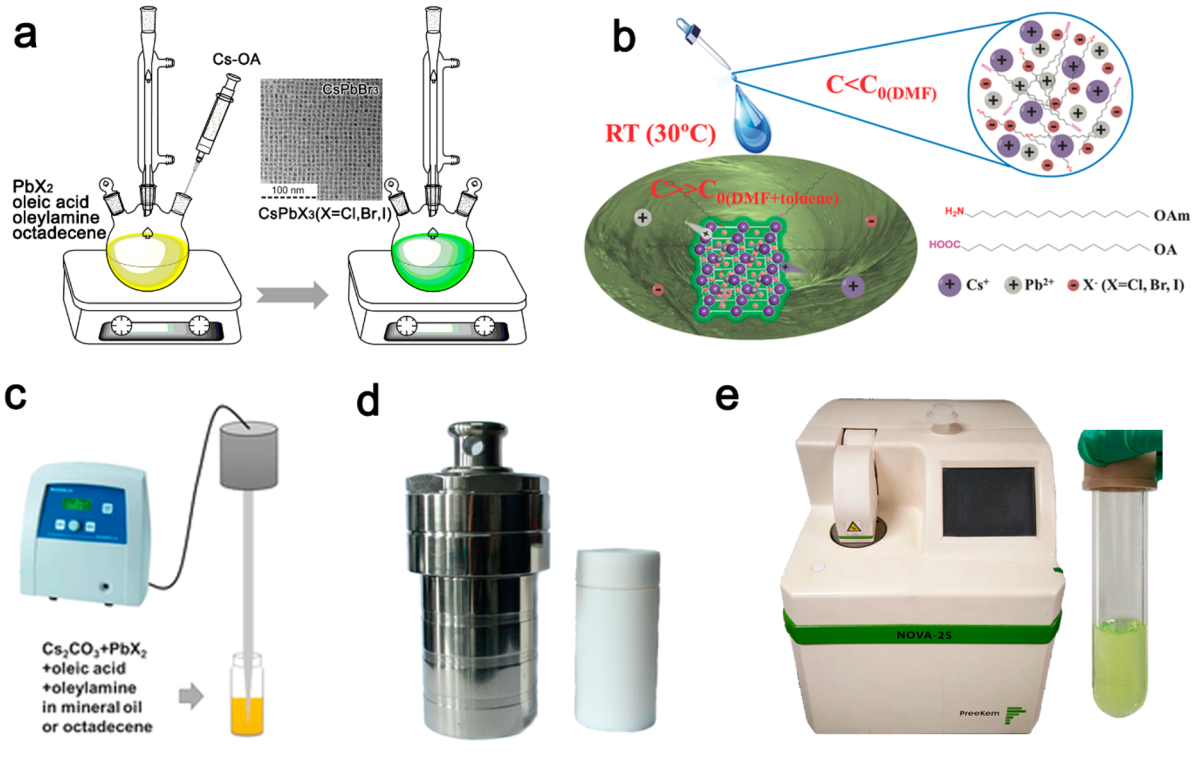

Figure 1. Schematic illustration of the methods for the synthesis of colloidal perovskite nanocrystals: (a) hot-injection method, (b) supersaturated recrystallization method, (c) ultrasonication-assisted method, (d) solvothermal method, and (e) microwave-assisted method. The images were modified with permission from refs (a) 14, (b), 18, (c) 19, (d) 21, and (e) 22.

photophysical properties of $CsPbX_3$ NCs are also excellent: they show high photoluminescence quantum yields (PLQYs, up to 90% without any post-treatment), wide color gamut (up to 140%), and narrow photoluminescence emission line-widths that can be easily tuned over the entire visible spectral region by manipulating the halide composition. For the traditional II−VI or III−V semiconductor NCs, it has been well-established that the particle size strongly affects their emission peak, which often brings problems in the consistency of the optical property as the particle size may vary from batch to batch during practical synthesis of such NCs. In contrast, much higher consistency in the optical property can be obtained in $CsPbX_3$ NCs because their emission peak position is mainly determined by the halide composition. With the advantages mentioned above, $CsPbX_3$ NCs have been regarded as promising materials for next-generation optoelectronic applications, as made evident by the emergence of over a thousand relevant papers in the past three years.[17]

In this Outlook, we first briefly summarize the recent advances in the field of IHP NCs, followed by our thoughts on the future directions of this field.

SYNTHETIC STRATEGIES AND MORPHOLOGY CONTROL

The Kovalenko group first reported the all-inorganic metal halide perovskite NCs in 2015,[14] which represents the launch of a new field in luminescent nanomaterials. As depicted in Figure 1a, a typical synthesis to colloidal $CsPbX_3$ NCs involves simply the injection of Cs-oleate into a three-neck flask containing an octadecene solution of predissolved PbX_2 at 140−200 °C. Several seconds later, monodisperse $CsPbX_3$ nanocubes, as shown in the inset of Figure 1a, are obtained after a rapid cooling down of the reaction system using an ice bath. The $CsPbX_3$ NCs show widely tunable emission wavelength (410−700 nm), high PLQY (up to 90%), narrow-emission line-widths (12−42 nm), and wide color gamut (up to 140% of NTSC standard). This method is similar to the synthesis of traditional II−VI and III−V semiconductor quantum dots (QDs), where high temperature and inert gas protection are usually required to improve the crystallinity of the product.

Compared with traditional II−VI and III−V semiconductor NCs such as metal chalcogenides and pnictides, the chemical bonding of $CsPbX_3$ NCs is more ionic. In principle, $CsPbX_3$ NCs can be prepared in a less stringent environment. It was soon discovered by many groups that high-quality $CsPbX_3$ NCs can be produced under moderate synthetic conditions, for example, at room temperature and ambient condition. Zeng and co-workers reported a ligand-assisted reprecipitation method, where Cs^+, Pb^{2+}, and X^- ions were predissolved in a polar solvent and then injected into a nonpolar solvent, leading to rapid nucleation and growth processes (Figure 1b).[18] This method can produce gram-scale $CsPbX_3$ NCs and, more importantly, avoid the need for inert gas protection and high temperature. This work was quickly followed by the development of many more facile, low-cost, and large-scale synthetic strategies to the preparation of high-quality $CsPbX_3$ NCs. For instance, Polavarapu et al. demonstrated that highly luminescent $CsPbX_3$ NCs could be prepared through an ultrasonication approach (Figure 1c).[19,20] Zhang et al. have developed solvothermal (Figure 1d)[21] and microwave-assisted (Figure 1e)[22] methods to synthesize $CsPbX_3$ NCs efficiently under air. Some postsynthetic methods have also been developed to produce $CsPbX_3$ NCs. In fact, there are several members in the cesium lead halide family, including $CsPbX_3$, Cs_4PbX_6, and

DOI: 10.1021/acscentsci.8b00201
ACS Cent. Sci. 2018, 4, 668−679

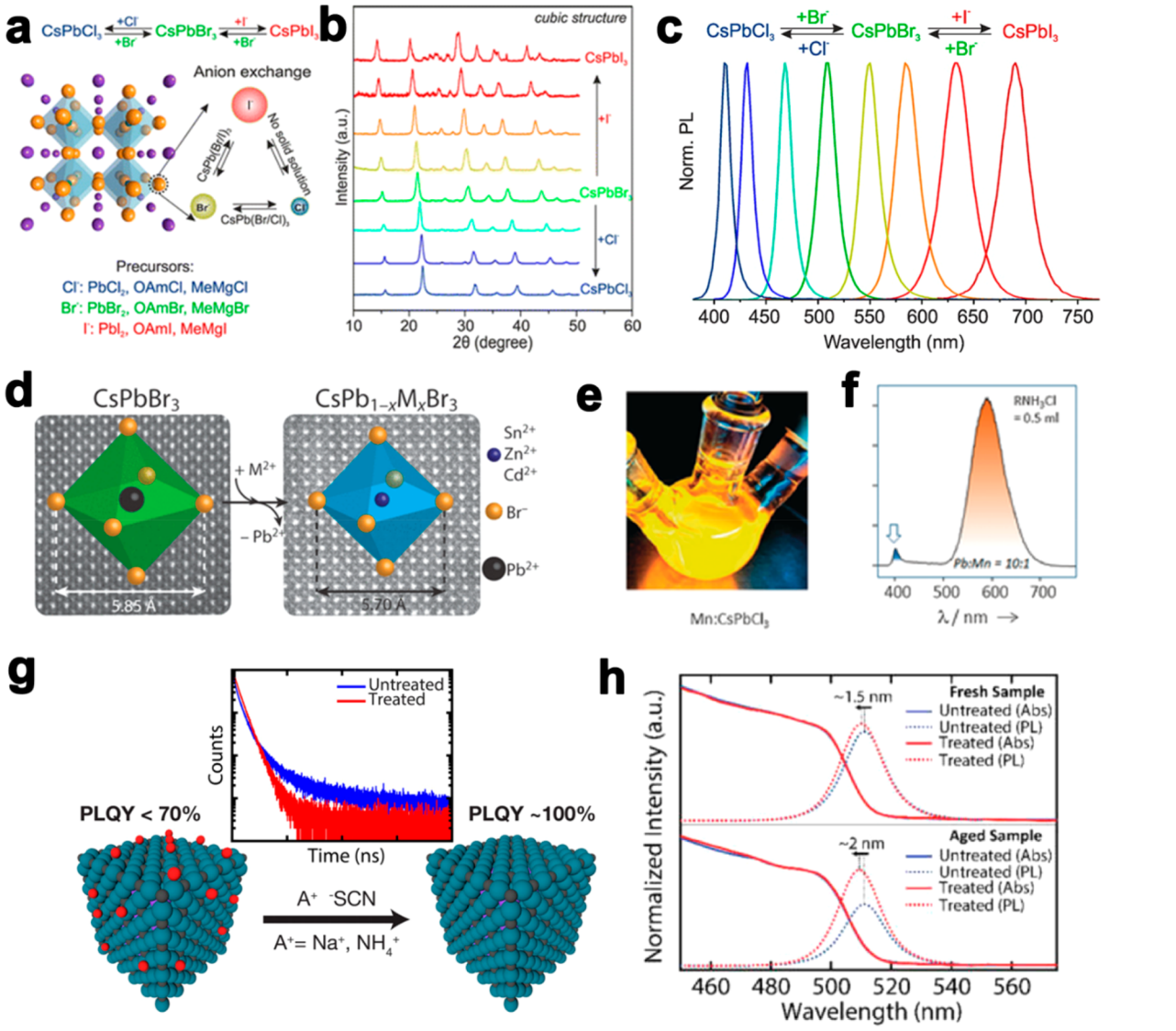

Figure 2. (a) Schematic illustration of the anion-exchange process within the cubic $CsPbCl_3$ NCs. (b) The XRD patterns indicate similar crystallite size before and after anion exchange. (c) Bright emission covering the entire visible spectral region can be realized with the anion-exchange approach. Images were modified with permission from ref 47. (d) Schematic illustration of partial replacement of Pb^{2+} with divalent cations. Images were modified with permission from ref 49. (e) Digital image and (f) PL spectra showing bright yellow emission of Mn^{2+}-doped $CsPbCl_3$ nanocrystals. Images were modified with permission from ref 51. (g, h) PLQY of $CsPbBr_3$ can be improved to near 100% by postsynthetic surface treatment using thiocyanate. Images were modified with permission from ref 53.

$CsPb_2X_5$. Although it is still under debate about which one is photoluminescent, an interesting transformation among the three phases has been noticed. Alivisatos et al. reported that $CsPbX_3$ could be transformed to nonluminescent Cs_4PbX_6 NCs after being treated with an excessive amine.[23] Manna et al. pointed out that Cs_4PbX_6 NCs could be regarded as a lead-deficit structure, which can be converted to $CsPbX_3$ by treating Cs_4PbX_6 with excessive PbX_2.[24] Meanwhile, we recently considered Cs_4PbX_6 NCs as a CsX-rich structure.[25] Because of the high solubility of CsX in water, nonluminescent Cs_4PbX_6 NCs can be converted to highly luminescent $CsPbX_3$ NCs by treating Cs_4PbX_6 NCs with water through a CsX-stripping process. $CsPbBr_3$ nanocubes can also be converted to $CsPb_2Br_5$ nanosheets with the assistance of dodecyl dimethylammonium bromide (DDAB).[26]

It has been well-established that the morphologies of nanomaterials might affect their properties greatly. Much effort has therefore been devoted to preparing $CsPbX_3$ NCs with different morphologies, including nanocubes,[14,27,28] nanowires,[29−33] nanospheres,[34,35] nanorods,[35,36] nanoplate,[37−40] two-dimensional nanosheets,[41−43] and so on. Cubelike $CsPbX_3$ NCs are the most common morphology among reported works. Their formation may be attributed to two major factors. First, $CsPbX_3$ is usually cubic or orthorhombic phase with near-cubic crystal lattice. On the other hand, the fast anion mobility of ionic $CsPbX_3$ and fast reaction kinetics make it challenging to realize oriented growth. Low-dimensional $CsPbX_3$ NCs tend to be prepared at a low reaction temperature. For example, precise control over the thickness of the platelike structure has been achieved at a lower reaction temperature. Alivisatos et al. reported that $CsPbX_3$ nanoplates with a thickness ranging from one to several layers could be obtained when the reaction temperature was kept low (90−130 °C),[44] although the product was a mixture of nanoplates with

DOI: 10.1021/acscentsci.8b00201
ACS Cent. Sci. 2018, 4, 668−679

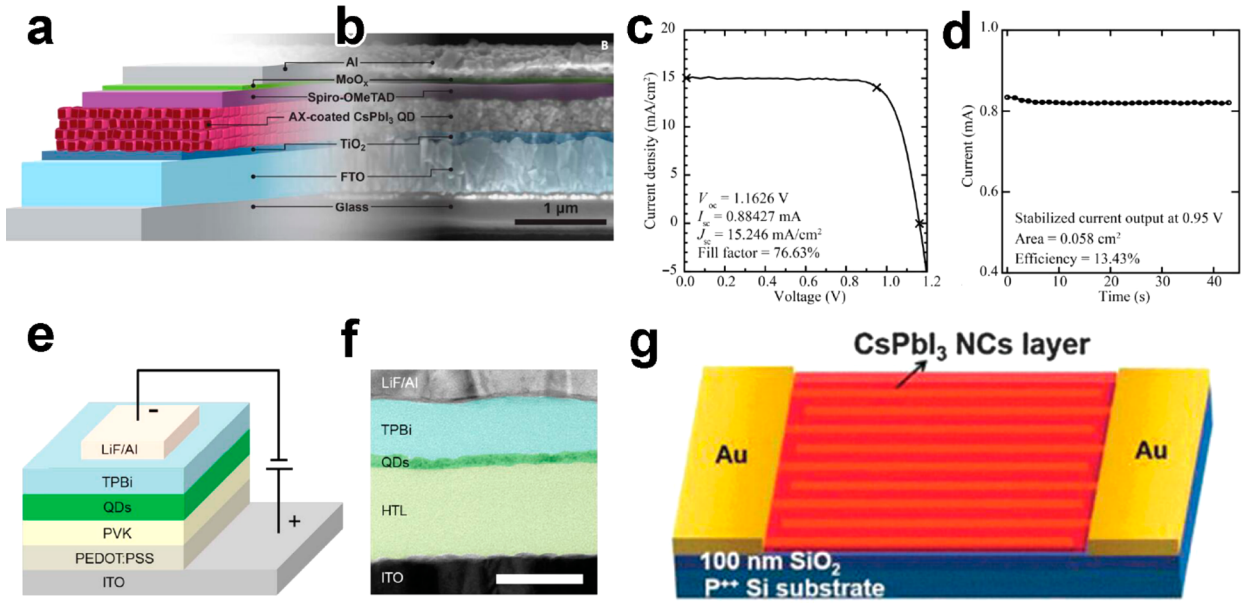

Figure 3. (a) Schematic illustration and (b) SEM image of the cross-section of a solar cell device. (c) NREL-certified *J*−*V* characteristics from forward bias to reverse bias. (d) NREL-certified stabilized current at a constant voltage of 0.95 V. Images were modified with permission from ref 56. (e) Schematic illustration and (f) cross-sectional TEM image of an LED device. Images were modified with permission from ref 27. (g) Schematic illustration of the first $CsPbI_3$ NCs photodetector. Images were modified with permission from ref 61.

various thicknesses. Recently, Zhang and co-workers found that simply heating the premixed precursors to the desired temperature (80−160 °C) could lead to the formation of $CsPbBr_3$ nanoplates with a uniform thickness.[40] The thickness of nanoplates could be precisely tuned from single layer to several layers by controlling the reaction temperature, with a higher temperature resulting in thicker nanoplates. As the thickness of nanoplates is smaller than the Bohr radius (~3.5 nm) of $CsPbBr_3$, a blue emission could be observed. Meanwhile, the edge length could be varied by tuning the reaction time, with a longer reaction time leading to a larger edge length. Ligands were found to also play an essential role in the morphology control. Deng et al. reported a reprecipitation method to the synthesis of $CsPbX_3$ nanocubes, nanospheres, nanorods, and nanoplatelets using ligands with different lengths of alkyl chains.[35]

Optical Properties. $CsPbX_3$ NCs have been considered as one of the most promising materials in optoelectronic devices and other related fields, mainly because their optical properties are intrinsically different from those of other nanostructured luminescent materials. For example, without any surface treatment, $CsPbX_3$ NCs can exhibit high PLQY and narrow-emission fwhm, while surface engineering is usually critical for traditional II−VI and III−V semiconductor quantum dots. More importantly, the PL emission of traditional metal chalcogenide and pnictide QDs is extremely sensitive to their particle size, leading to poor optical consistency for materials synthesized in different batches. In contrast, the PL peak position of $CsPbX_3$ NCs is determined mainly by their halide composition. As reported by Kovalenko et al.,[14] the PL emission of $CsPbX_3$ NCs can cover the full visible range (410−700 nm) when different halide precursors were used. This approach has proven to be a convenient and highly reproducible way to determine the optical properties in comparison with the traditional size-controlled method.

The PL peak position of $CsPbX_3$ NCs can also be simply realized through post-chemical-transformation (Figure 2a−c).[45−47] Because of the high charge carrier mobility, the halide ions can be replaced partially or completely by each other. As demonstrated by the Kovalenko group, the anion-exchange process could be achieved in a fast and facile manner.[47] The bright PL emission could be tuned to cover the entire visible range (410−700 nm) by treating presynthesized $CsPbX_3$ NCs with different amounts of other halide ions at room temperature. Interestingly, the morphology of the NCs could be well-maintained. The PLQYs were also maintained (20−80%), with narrow-emission line-widths (10−40 nm). In addition to the above-mentioned anion-exchange method, quantum-confinement-effect-induced PL spectra variation has also been observed when the dimension of NCs was smaller than their Bohr radius (~2.5 nm for $CsPbCl_3$, 3.5 nm for $CsPbBr_3$, and 6.0 nm for $CsPbI_3$).[14,37,48] Doping $CsPbX_3$ NCs with divalent cations (such as Zn^{2+}, Cd^{2+}, Mn^{2+}) represents another efficient and effective way to tune their optical properties.[49−52] For example, when Mn^{2+} ions were incorporated into wide-band-gap $CsPbCl_3$ and $CsPb(Cl/Br)_3$ NCs, the d−d transition of Mn^{2+} could cause strong yellow−orange emission (Figure 2e,f).[51]

In addition to the composition-dependent PL emission, another very attractive optical property of $CsPbX_3$ NCs is the tolerance of ultrahigh density of defects (up to 1−2 atom %, typical as vacancies), which is much higher than conventional binary compound QDs, resulting in high PLQY without the need of any surface treatment. To improve the PLQY of traditional metal chalcogenide and pnictide QDs, one may use another semiconductor with a wider band gap as the shell material to passivate the surface. Because of the low stability of the ionic $CsPbX_3$ NCs, it has been very difficult to achieve such surface passivation. Some progress has been achieved by modifying the synthetic strategies or post-treatment with other compounds. For example, Alivisatos et al. reported that thiocyanate treatment could dramatically promote the PLQY of $CsPbBr_3$ NCs from 70% to nearly 100% (Figure 2g,h).[53] In this case, thiocyanate passivates the lead-rich surface,

DOI: 10.1021/acscentsci.8b00201
ACS Cent. Sci. 2018, 4, 668−679

diminishing the shallow electron traps of $CsPbBr_3$ NCs. Recently, Shen et al. prepared $CsPbI_3$ NCs with up to 100% PLQY by using organo-lead trioctylphosphine-PbI_2 as the precursor.[54]

Application. Thanks to their exciting photophysical properties, $CsPbX_3$ NCs have been utilized in many photoelectric devices, including solar cells, light-emitting diodes (LEDs), photodetectors, and lasers. In particular, $CsPbX_3$ NCs are promising candidates in the field of solar cells. The PCE of $CsPbX_3$-based solar cells has grown rapidly over the past several years. In 2016, Luther et al. reported a solar cell based on phase-stable α-$CsPbI_3$ QDs with a PCE of about 10.77%.[55] Later, a record-high PCE of 13.43% was achieved through an A-site cation halide salt (AX) treatment (Figure 3a–d).[56] Zhao et al. reported a solar cell of PCE of 11.8% with high phase stability at room temperature for months and at 100 °C for over 150 h.[57] In addition to the rising performance, the important advantages of $CsPbX_3$-based solar cells also include higher thermal stability compared with OHP-based solar cells. As confirmed by Cahen et al., the performance of $CsPbX_3$-based solar cells can be maintained for up to 2 weeks under constant illumination, which is much better than that of OHP-based solar cells.[58] Although much progress has been made, currently the PCE of IHP-based solar cells is still much lower than that of OHP-based solar cells. How to further improve the efficiency of IHP-based solar cells remains a quite challenging question.

Zeng et al. demonstrated the first application of $CsPbX_3$ NCs in LEDs.[27] The structure of the device is illustrated in Figure 3e,f. The color of LEDs can be tuned from blue to orange by adjusting the content and the category of anions. However, the external quantum efficiency (EQE) of the first reported $CsPbBr_3$ LED was only 0.12%. The low EQE of $CsPbX_3$-based LEDs could be attributed to the excessive ligands that form an insulating layer. To solve this problem, Zeng et al. developed a new method to control the ligand density and balance the surface passivation and carrier injection. The EQE has been promoted to 6.27%.[59] More recently, Chiba et al. reported a novel washing process using an ester solvent to remove excess ligands and achieved the highest EQE (8.73%) of $CsPbBr_3$-based LED devices.[60]

The photodetector is another exciting application of IHP NCs. The first reported IHP-based photodetector was made by Ramasamy et al.[61] As illustrated in Figure 3g, $CsPbI_3$ NCs were used as the main component. A very good on/off photocurrent ratio of 10^5 was achieved by using the very simple device. This work opened a new door to the application of IHP NCs. After that, much effort has been devoted to improving the performance of IHP-NC-based photodetectors. For example, Zeng et al. developed a room-temperature healing method to treat $CsPbBr_3$ film, resulting in significantly improved performance of photodetectors.[62] In addition to the cubelike structure, $CsPbX_3$ NCs with different morphologies, such as nanorods[63] and nanosheets,[41,64] have also been used to improve the performance by utilizing their unique feature in charge carrier transfer. Overall, the reports on the IHP-based photodetectors are limited, and more efforts are still needed to improve the performance.

Because of their high absorption coefficient and low density of defects, IHP NCs have also been used to fabricate lasing devices.[65−67] For example, Sun et al. first reported the potential application of $CsPbX_3$ QDs in lasers.[67] Xiong et al. prepared high-quality $CsPbX_3$ nanoplates through a vapor-phase van der Waals epitaxy method,[65] and then used the well-defined product for lasing. They were able to realize multicolor and low-threshold lasing, and obtained so far one of the highest values of mode line-width (0.14−0.15 nm). Despite these achievements, the stability and the excitation mechanism are still quite challenging problems to be addressed.

OUTLOOK

As summarized above, intensive efforts have been made in the development of all-inorganic metal halide perovskite nanomaterials since the first study in 2015.[14] Significant progress has been achieved in the controlled preparations of IHP NCs and optimizations of their properties over the past three years. Their promising applications in different areas have also been partially demonstrated. Despite these great successes, the research in this field is still in its early infancy. Several issues must be addressed before the widespread practical applications of IHP NCs become possible. In this section, we discuss our perspectives regarding challenges and future research in this area.

Stability Issue. Presumably, the most prominent issue with IHP NCs is still their structural stability against chemical (particularly moisture), thermal, and photodisturbances. For example, the colloidal stability of IHP NCs is often questionable because of the relatively weak binding of common ligands to the particle surface. Acids and amines with long alkyl chains, such as oleic acid and oleylamine, are the most widely used ligands for the synthesis of IHP NCs. These ligands can nevertheless easily detach themselves from the nanocrystal surface, leading to the aggregation and structural damage of IHP NCs. New ligand chemistry is therefore needed. Recently, Sun et al. attempted to address this issue by replacing traditional oleic acid/olelyamine with octylphosphonic acid (OPA) and found that the stability of $CsPbX_3$ NCs could be significantly enhanced.[68] Thanks to the relatively strong interaction between OPA and lead ions, the resulting $CsPbX_3$ NCs remained highly photoluminescent after eight purification cycles. It was found that OPA could provide much better protection even in the presence of fewer ligands on $CsPbX_3$ NC surfaces (only ∼4.6% ligand left in the OPA-$CsPbX_3$ system in comparison with ∼29.7% for OA/OLA-$CsPbBr_3$). As a result, the EQE of the LED device has been promoted to 6.5% (Figure 4a). Wu and co-workers also found that the addition of trioctylphosphine oxide (TOPO) into the oleic acid/oleylamine system can significantly improve the stability of IHP NCs against antisolvent cleaning.[69]

Zwitterionic ligands that possess several anchoring groups can also provide effective protection for IHP NCs (Figure 4b).[70] Compared with conventional acids and amines, zwitterionic ligands show stronger adhesion to the surface of IHP NCs via special chelating effect. Ligand exchange on presynthesized IHP NCs is another effective way to passivate the surface of NCs. Bakr et al. reported that both the PLQY and stability of $CsPbX_3$ NCs could be dramatically improved after ligand exchange with didodecyl dimethylammonium bromide and bidentate 2,2′-iminodibenzoic acid.[71,72] Recently, it has been found that anchoring $CsPbBr_3$ NCs onto a substrate can improve their stability. By using a presynthesized aminated silica sphere as the substrate, Zeng et al. successfully grew $CsPbBr_3$ NCs on the silica spheres.[73] Since all NCs are anchored on the surface of silica, photoinduced regrowth and deterioration of NCs were inhibited, leading to enhanced stability against moisture and light exposure.

DOI: 10.1021/acscentsci.8b00201
ACS Cent. Sci. 2018, 4, 668−679

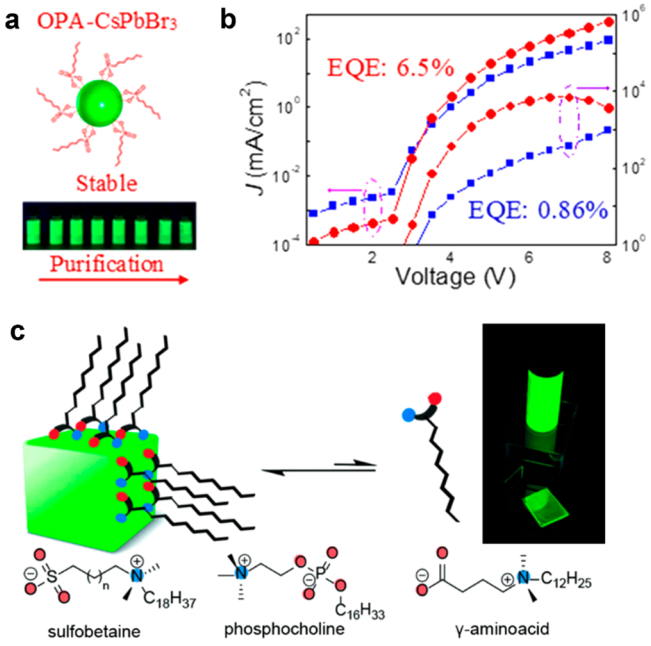

Figure 4. (a) Schematic structure of OPA-capped $CsPbBr_3$ NCs. (b) *J*–*V*–*L* curve of devices based on different ligands (blue line for OA/OLA-capped $CsPbBr_3$ NCs, and red line for OPA-capped $CsPbBr_3$ NCs). Images were modified with permission from ref 68. (c) Schematic structure of $CsPbBr_3$ NCs capped by long-chain zwitterionic molecules. Images were modified with permission from ref 70.

In addition to the surface passivation with organic ligands, another way of improving the stability of IHP NCs is to encapsulate these vulnerable NCs into a stable and inert shell made of different materials, such as graphene, silica, amorphous alumina matrix, and polymer.[74−81] For example, after encapsulation within silica/alumina monolith, $CsPbBr_3$ NCs showed much higher stability against light irradiation than naked ones (Figure 5a−c).[81] Although researchers have proposed some strategies to maintain the original properties of IHP NCs after the encapsulation, there are still several major questions.

First, how to modify IHP NCs with another material on a single-particle level is still a big challenge. In many applications, e.g., cell labeling, small particles are preferred. In the examples mentioned above, many IHP NCs were encapsulated together into the shell material, resulting in very large particles (several hundred nanometers to several micrometers in size). All of the reported IHP NCs are hydrophobic because their surfaces are covered with long-alkyl-chain ligands. Since most of the reported shell materials are hydrophilic, it is challenging to grow hydrophilic materials onto the hydrophobic surface directly. Recently, for the first time, we found that Janus $CsPbX_3$/oxide (SiO_2 and Ta_2O_5) nanoparticles can be obtained through an interfacial synthesis process,[82] in which presynthesized Cs_4PbX_6 NCs and oxide precursors were mixed in hexane and then treated with water. At the water/hexane interface, Cs_4PbX_6 NCs were converted to $CsPbX_3$ NCs through a CsX-stripping process because of the high solubility of CsX in water.[25] Meanwhile, the hydrophobic ligands were removed during the stripping process, leaving a hydrophilic surface to the environment. Simultaneously, the hydrolysis of oxide precursor happened at the interface, leading to the formation of Janus NCs (Figure 5d−f). Thanks to the surface modification, the as-prepared Janus nanoparticles showed improved stability in air (Figure 5g). However, how to achieve a full coating of IHP NCs on a single-particle level remains a challenge to be addressed.

Second, how to coat IHP NCs with a stable and active shell is a problem. For traditional II−VI or III−V semiconductor NCs, encapsulating them into an active and more stable shell can not only improve the stability, but also tune the photophysical properties. One of the most widely used shell materials is ZnS.[83] However, most of the reported shell materials for IHP NCs are organic or amorphous materials. No full coating of IHP NCs into an active layer has been reported. This question can be partially attributed to the hydrophobic surface we have discussed above. On the other hand, the strong interaction between Pb and chalcogen anions (S^{2-}, Se^{2-}, or Te^{2-}) prevents the coating of the metal chalcogenide. To achieve such kind of coating, developing some sandwich-like structures might be a plausible approach, in which an ultrathin inert shell could be coated onto the surface of IHP NCs first, followed by the coating of the metal chalcogenide layer (Figure 6). By engineering the thickness and composition of the middle layer, the photophysical properties might also be tuned. Semiconductors, oxides, and polymers are promising shell materials to protect IHP NCs. With the protection of shell materials, the IHP NCs could be dispersed into water or other polar solvents. More importantly, the toxicity can be minimized by the core−shell configuration. These advantages may bring new opportunities to IHP NCs in some important applications, such as LCD displays, photocatalysis, and cell imaging.

Toxicity of Lead. The toxicity of lead is another inescapable problem of IHP before industrialization. So far, some progress has been achieved in the preparation of environmentally friendly IHPs by replacing lead with low-toxicity or nontoxic metal, such as tin, bismuth, and antimony. For example, $CsSnX_3$ has been considered as a promising alternative, which exhibits different properties due to the introduction of Sn.[84−86] Orthorhombic $CsSnI_3$ NCs reported by Kanatzidis et al. not only show the properties of a p-type direct band gap but also possess high hole mobility, which come from the intrinsic defects associated with Sn vacancies.[87] However, the development and application of $CsSnI_3$ NCs have been limited seriously by their poor stability as they are extremely sensitive to moisture, oxygen, and thermal treatment. What's worse, its PLQY (<1%) is too low to meet the requirement for practical applications. $Cs_3Bi_2X_9$ and $Cs_3Sb_2X_9$ NCs have also been successfully synthesized, which exhibited much higher PLQY compared to $CsSnX_3$ (Figure 7a−c). However, the PL spectra can cover only part of the visible range (350−560 nm).[88−91] Novel lead-free double-perovskite NCs, such as Cs_2AgBiX_6 and Cs_2InAgX_6 NCs,[92−94] have been successfully obtained, which provide new members for the development of perovskite materials (Figure 7d−f). In general, however, these lead-free IHP NCs have lower efficiency compared with lead-based ones. It is still urgently needed to develop new lead-free materials with high performance or find effective means to improve the performance of the current ones. The rapid development of computational chemistry might be able to offer hints to the rational design of more potential candidates. Zhao et al. exploited lead-free halide perovskite materials using first-principle calculations. Some double-perovskite structures, such as $Cs_2InSbCl_6$ and $Cs_2InBiCl_6$, have been regarded as promising materials for stable and efficient candidates for the application of solar cells.[95]

DOI: 10.1021/acscentsci.8b00201
ACS Cent. Sci. 2018, 4, 668−679

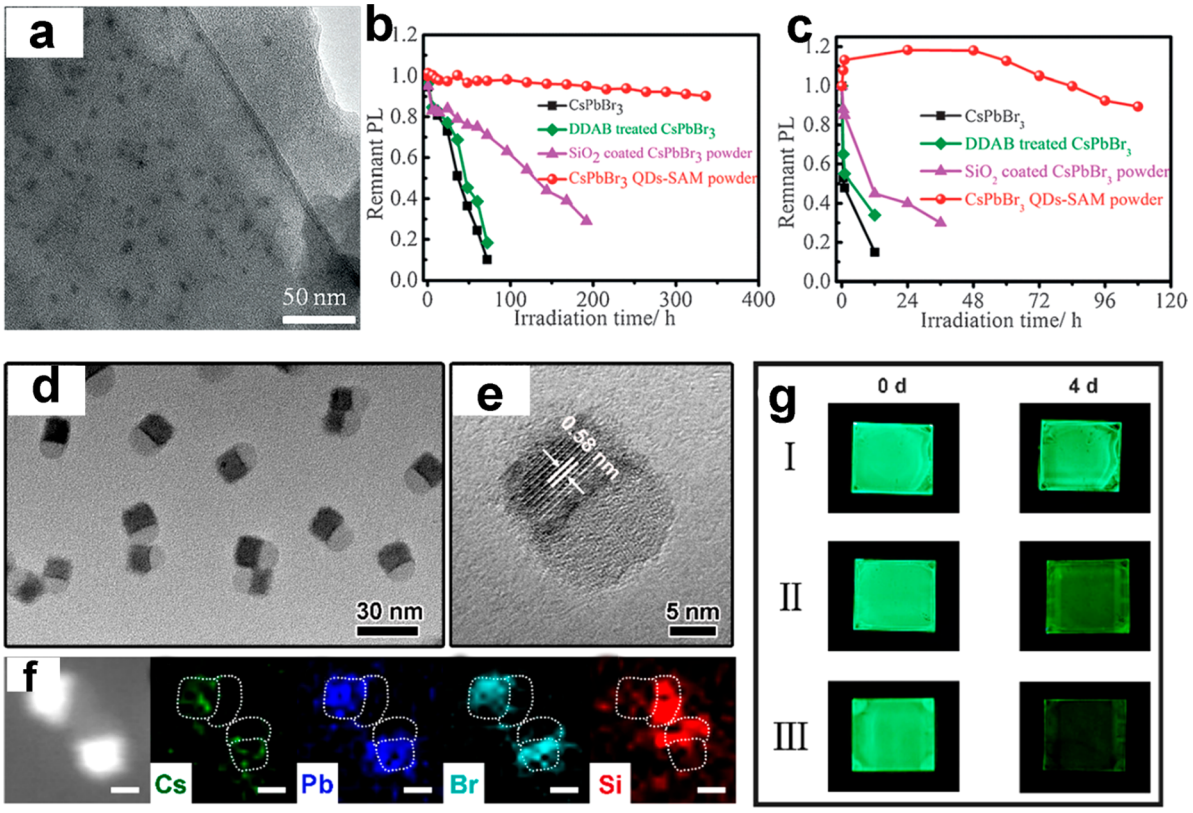

Figure 5. (a) TEM images of $CsPbBr_3$ NCs-silica/alumina monolith (SAM). Photostability of the $CsPbBr_3$ QDs-SAM powder (b) under illumination with a 470 nm LED light and (c) sealed with PDMS on the LED chip (5 mA, 2.7 V). The images were modified with permission from ref 81. (d) TEM image of the obtained $CsPbBr_3/SiO_2$ Janus NCs. (e) HRTEM image of a single $CsPbBr_3/SiO_2$ NC. (f) HAADF-STEM image and elemental mapping images. (g) Photographs of (I) $CsPbBr_3/SiO_2$ NCs, (II) WT-$CsPbBr_3$ NCs, and (III) HI-$CsPbBr_3$ NCs thin film stored in humid air (40 °C and humidity of 75%). The images were modified with permission from ref 82.

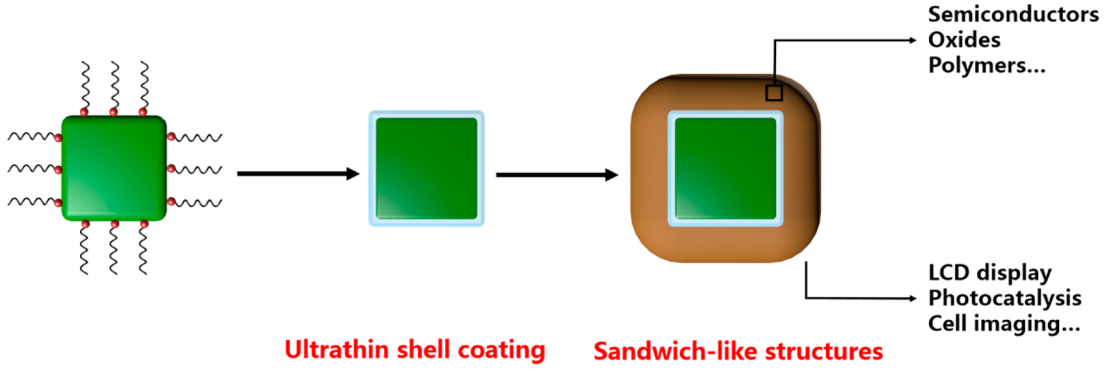

Figure 6. Schematic illustration of the design of sandwich-like structures with possible shell materials and promising applications.

Photocatalysis. The potential application of IHP NCs in photocatalysis is another very attractive topic because of their excellent photophysical properties, including tunable band gap, high absorption coefficient, broad absorption spectrum, high charge carrier mobility, and long charge diffusion lengths. Kuang and co-workers reported that $CsPbBr_3$ NCs could be used to trigger the photocatalytic reduction of CO_2 in ethyl acetate (Figure 8a,b),[96] and observed relatively good stability. More importantly, a 25.5% increase in the catalytic performance has been observed when $CsPbBr_3$ NCs were combined with graphene oxide. The improved performance has been attributed to the enhanced electron extraction and transport. Recently, lead-free IHP NCs have also been used for photocatalytic reduction of CO_2. By adopting a similar reaction

The potential application of IHP NCs in photocatalysis is another very attractive topic because of their excellent photophysical properties, including tunable band gap, high absorption coefficient, broad absorption spectrum, high charge carrier mobility, and long charge diffusion lengths.

DOI: 10.1021/acscentsci.8b00201
ACS Cent. Sci. 2018, 4, 668−679

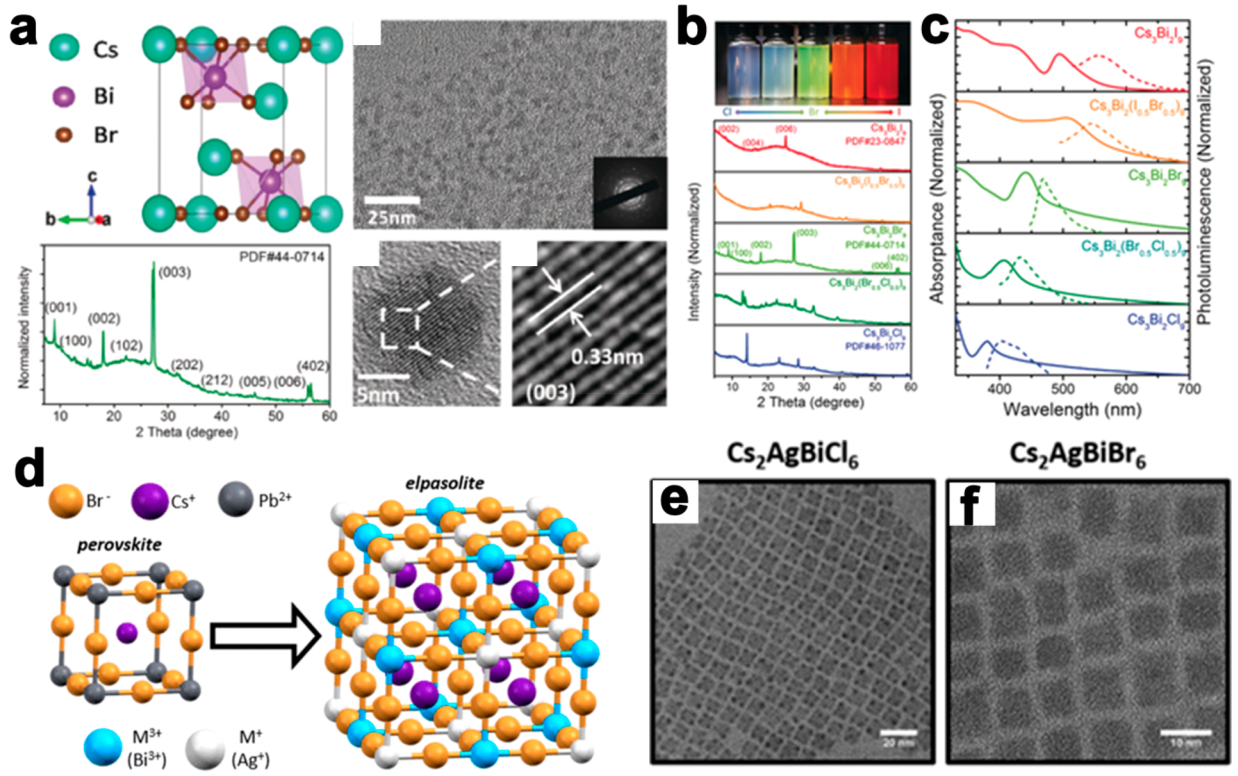

Figure 7. (a) $Cs_3Bi_2Br_9$ unit cell, XRD patterns of $Cs_3Bi_2Br_9$ NCs, and TEM image of $Cs_3Bi_2Br_9$ NCs. (b) Photographs of as-obtained colloidal $Cs_3Bi_2X_9$ and XRD patterns of NCs containing pure and mixed halides. (c) Steady-state absorption and PL spectra of NCs containing pure and mixed halides. The images were modified with permission from ref 88. (d) Structure of $Cs_2AgBiBr_6$. (e) TEM image of $Cs_2AgBiCl_6$ NCs. (f) TEM image of $Cs_2AgBiBr_6$ NCs. The images were modified with permission from ref 93.

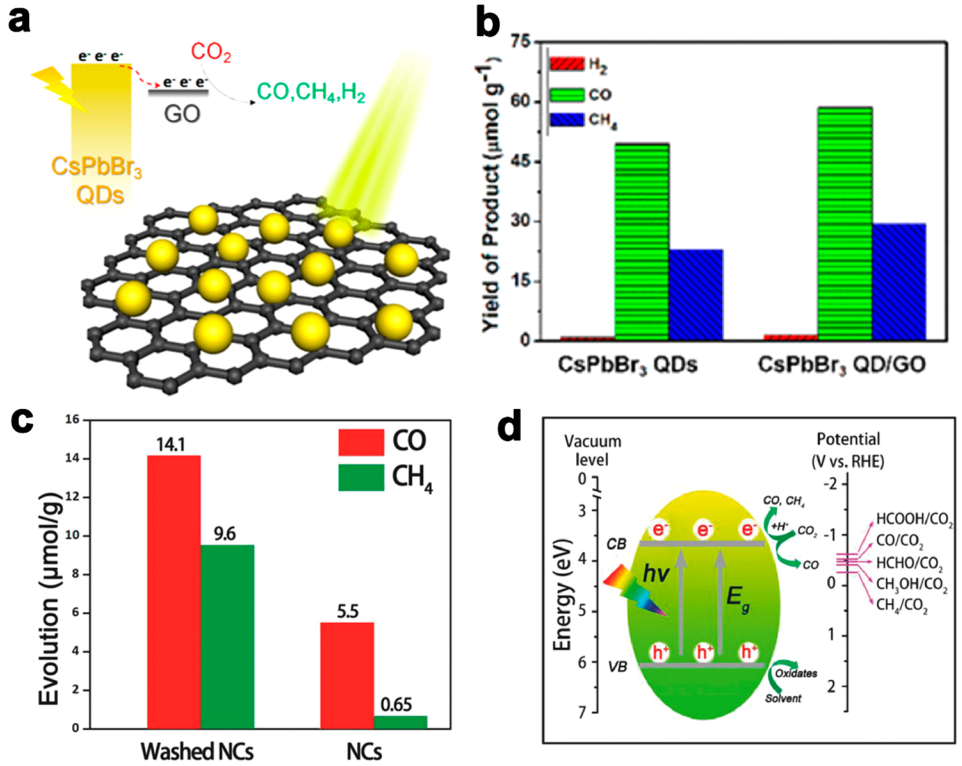

Figure 8. (a) Schematic illustration of CO_2 photoreduction over the $CsPbBr_3$ QD/GO photocatalyst. (b) Catalytic performance of $CsPbBr_3$ QD and $CsPbBr_3$ QD/GO. The images were modified with permission from ref 95. (c) Catalytic performance of $Cs_2AgBiBr_6$ NCs in CO_2 reduction. (d) Schematic illustration of the photoreduction of CO_2 over $Cs_2AgBiBr_6$ NCs. The images were modified with permission from ref 92.

DOI: 10.1021/acscentsci.8b00201
ACS Cent. Sci. 2018, 4, 668−679

system, $Cs_2AgBiBr_6$ NCs were used as the photocatalysts (Figure 8c,d).[92] Although the photocatalytic performance is still poor compared to other reported semiconductor catalysts, this work demonstrates the vast potential of IHP NCs in environmentally friendly photocatalysis.

Despite the successful demonstration of IHP NCs in photocatalysis, there is still a long way to go toward practical applications. First, the recombination rate of photogenerated charge carriers in IHP NCs is high, leading to low utilization efficiency of electrons and poor performance. Second, the low stability of IHP NCs in frequently used polar media such as water and alcohol is still the biggest problem. For example, compared to nonaqueous ethyl acetate, water is a much better reaction medium for CO_2 reduction or other photocatalysis reactions. However, none of the reported IHP NCs can be dispersed in water so far. Additionally, when carbon-containing nonpolar solvents were used as the reaction media, CO or CH_4 might be generated from the solvents rather than from the photocatalytic reaction, causing big trouble in the productivity calculation. One unexplored but possible way to overcome these challenges is to modify such IHP NCs with wide-band-gap materials or metal NCs that can form hetero- or core−shell nanostructures. In this way, the stability might be improved, and the charge separation and the catalytic performance could be enhanced.

CONCLUSION

In this Outlook, we have introduced all-inorganic metal halide perovskite nanocrystals as a special class of semiconductor materials that inherit the excellent optical and electronic properties of organic perovskite materials, including tunable band gap, high absorption coefficient, broad absorption spectrum, high charge carrier mobility, and long charge diffusion lengths. Compared with OHP, these IHP materials exhibit high melting point, enhanced thermostability, and photostability. These unique features of IHP NCs hold great promise for practical applications in solar cells, photodetectors, light-emitting diodes, and lasers, among others. Despite the recent progress, the research in this field is still in its early infancy. Many challenges, especially stability, toxicity, and synthesis, should be addressed before IHP materials can be considered for practical application. This is an emerging and exciting area that may greatly impact the semiconductor industry and our daily life in the near future. We hope this Outlook may bring together researchers from various areas to explore many interesting aspects of this new type of material.

Many challenges, especially stability, toxicity, and synthesis, should be addressed before IHP materials can be considered for practical application.

AUTHOR INFORMATION

Corresponding Author

*E-mail: yadongy@ucr.edu.

ORCID

Qiao Zhang: 0000-0001-9682-3295

Yadong Yin: 0000-0003-0218-3042

Author Contributions

The manuscript was written through contributions of all authors. All authors have given approval to the final version of the manuscript.

Notes

The authors declare no competing financial interest.

ACKNOWLEDGMENTS

This work is supported by the Ministry of Science and Technology of the People's Republic of China (2016YFE0129600), and National Natural Science Foundation of China (21673150, 21611540336). We acknowledge the financial support from the 111 Project, Collaborative Innovation Center of Suzhou Nano Science and Technology (NANO−CIC), the Priority Academic Program Development of Jiangsu Higher Education Institutions (PAPD), and SWC for Synchrotron Radiation Research. Acknowledgment is also made to the Donors of the American Chemical Society Petroleum Research Fund for partial support of this research (55904-ND10).

ABBREVIATIONS

OHP, organic metal halide perovskite; IHP, inorganic metal halide perovskite; NCs, nanocrystals; PLQYs, photoluminescence quantum yields; LED, light-emitting diode; NTSC, national television system committee; QDs, quantum dots

REFERENCES

(1) Yoshikawa, K.; Kawasaki, H.; Yoshida, W.; Irie, T.; Konishi, K.; Nakano, K.; Uto, T.; Adachi, D.; Kanematsu, M.; Uzu, H.; Yamamoto, K. Silicon heterojunction solar cell with interdigitated back contacts for a photoconversion efficiency over 26%. *Nat. Energy* **2017**, *2*, 17032.

(2) Kojima, A.; Teshima, K.; Shirai, Y.; Miyasaka, T. Organometal halide perovskites as visible-light sensitizers for photovoltaic cells. *J. Am. Chem. Soc.* **2009**, *131*, 6050−6051.

(3) Jeon, N. J.; Noh, J. H.; Yang, W. S.; Kim, Y. C.; Ryu, S.; Seo, J.; Seok, S. I. Compositional engineering of perovskite materials for high-performance solar cells. *Nature* **2015**, *517*, 476−480.

(4) Yang, W. S.; Park, B. W.; Jung, E. H.; Jeon, N. J.; Kim, Y. C.; Lee, D. U.; Shin, S. S.; Seo, J.; Kim, E. K.; Noh, J. H.; Seok, S. I. Iodide management in formamidinium-lead-halide-based perovskite layers for efficient solar cells. *Science* **2017**, *356*, 1376−1379.

(5) Christians, J. A.; Schulz, P.; Tinkham, J. S.; Schloemer, T. H.; Harvey, S. P.; Tremolet de Villers, B. J.; Sellinger, A.; Berry, J. J.; Luther, J. M. Tailored interfaces of unencapsulated perovskite solar cells for > 1,000 h operational stability. *Nat. Energy* **2018**, *3*, 68−74.

(6) Byun, J.; Cho, H.; Wolf, C.; Jang, M.; Sadhanala, A.; Friend, R. H.; Yang, H.; Lee, T.-W. Efficient visible quasi-2D perovskite light-emitting diodes. *Adv. Mater.* **2016**, *28*, 7515−7520.

(7) Seo, H.-K.; Kim, H.; Lee, J.; Park, M.-H.; Jeong, S.-H.; Kim, Y.-H.; Kwon, S.-J.; Han, T.-H.; Yoo, S.; Lee, T.-W. Efficient flexible organic/inorganic hybrid perovskite light-emitting diodes based on graphene anode. *Adv. Mater.* **2017**, *29*, 1605587.

(8) Wang, H.; Kim, D. H. Perovskite-based photodetectors: materials and devices. *Chem. Soc. Rev.* **2017**, *46*, 5204−5236.

(9) Fu, Y.; Zhu, H.; Schrader, A. W.; Liang, D.; Ding, Q.; Joshi, P.; Hwang, L.; Zhu, X. Y.; Jin, S. Nanowire lasers of formamidinium lead halide perovskites and their stabilized alloys with improved stability. *Nano Lett.* **2016**, *16*, 1000−1008.

(10) Zhu, H.; Fu, Y.; Meng, F.; Wu, X.; Gong, Z.; Ding, Q.; Gustafsson, M. V.; Trinh, M. T.; Jin, S.; Zhu, X. Y. Lead halide perovskite nanowire lasers with low lasing thresholds and high quality factors. *Nat. Mater.* **2015**, *14*, 636−642.

(11) Gu, C.; Lee, J. S. Flexible hybrid organic-inorganic perovskite memory. *ACS Nano* **2016**, *10*, 5413−5418.

DOI: 10.1021/acscentsci.8b00201
ACS Cent. Sci. 2018, 4, 668−679

(12) Leijtens, T.; Eperon, G. E.; Noel, N. K.; Habisreutinger, S. N.; Petrozza, A.; Snaith, H. J. Stability of metal halide perovskite solar cells. *Adv. Engergy Mater.* **2015**, *5*, 1500963.
(13) Choi, H.; Jeong, J.; Kim, H.-B.; Kim, S.; Walker, B.; Kim, G.-H.; Kim, J. Y. Cesium-doped methylammonium lead iodide perovskite light absorber for hybrid solar cells. *Nano Energy* **2014**, *7*, 80−85.
(14) Protesescu, L.; Yakunin, S.; Bodnarchuk, M. I.; Krieg, F.; Caputo, R.; Hendon, C. H.; Yang, R. X.; Walsh, A.; Kovalenko, M. V. Nanocrystals of cesium lead halide perovskites ($CsPbX_3$, X = Cl, Br, and I): novel optoelectronic materials showing bright emission with wide color gamut. *Nano Lett.* **2015**, *15*, 3692−3696.
(15) Divitini, G.; Cacovich, S.; Matteocci, F.; Cina, L.; Di Carlo, A.; Ducati, C. In situ observation of heat-induced degradation of perovskite solar cells. *Nat. Energy* **2016**, *1*, 15012.
(16) Sun, Q.; Yin, W.-J. Thermodynamic stability trend of cubic perovskites. *J. Am. Chem. Soc.* **2017**, *139*, 14905−14908.
(17) Kovalenko, M. V.; Protesescu, L.; Bodnarchuk, M. I. Bodnarchuk Properties and potential optoelectronicapplications of lead halide perovskite nanocrystals. *Science* **2017**, *358*, 745−750.
(18) Li, X.; Wu, Y.; Zhang, S.; Cai, B.; Gu, Y.; Song, J.; Zeng, H. $CsPbX_3$ quantum dots for lighting and displays: room-temperature synthesis, photoluminescence superiorities, underlying origins and white light-emitting diodes. *Adv. Funct. Mater.* **2016**, *26*, 2435−2445.
(19) Tong, Y.; Bladt, E.; Ayguler, M. F.; Manzi, A.; Milowska, K. Z.; Hintermayr, V. A.; Docampo, P.; Bals, S.; Urban, A. S.; Polavarapu, L.; Feldmann, J. Highly luminescent cesium lead halide perovskite nanocrystals with tunable composition and thickness by ultrasonication. *Angew. Chem., Int. Ed.* **2016**, *55*, 13887−13892.
(20) Tong, Y.; Bohn, B. J.; Bladt, E.; Wang, K.; Müller-Buschbaum, P.; Bals, S.; Urban, A. S.; Polavarapu, L.; Feldmann, J. From precursor powders to $CsPbX_3$ perovskite nanowires: One-pot synthesis, growth mechanism, and oriented self-assembly. *Angew. Chem., Int. Ed.* **2017**, *56*, 13887−13892.
(21) Chen, M.; Zou, Y.; Wu, L.; Pan, Q.; Yang, D.; Hu, H.; Tan, Y.; Zhong, Q.; Xu, Y.; Liu, H.; Sun, B.; Zhang, Q. Solvothermal synthesis of high-quality all-inorganic cesium lead halide perovskite nanocrystals: from nanocube to ultrathin nanowire. *Adv. Funct. Mater.* **2017**, *27*, 1701121.
(22) Pan, Q.; Hu, H.; Zou, Y.; Chen, M.; Wu, L.; Yang, D.; Yuan, X.; Fan, J.; Sun, B.; Zhang, Q. Microwave-assisted synthesis of high-quality "all-inorganic" $CsPbX_3$ (X = Cl, Br, I) perovskite nanocrystals and their application in light emitting diodes. *J. Mater. Chem. C* **2017**, *5*, 10947−10954.
(23) Liu, Z.; Bekenstein, Y.; Ye, X.; Nguyen, S. C.; Swabeck, J.; Zhang, D.; Lee, S. T.; Yang, P.; Ma, W.; Alivisatos, A. P. Ligand Mediated Transformation of Cesium Lead Bromide Perovskite Nanocrystals to Lead Depleted Cs4PbBr6 Nanocrystals. *J. Am. Chem. Soc.* **2017**, *139*, 5309−5312.
(24) Akkerman, Q. A.; Park, S.; Radicchi, E.; Nunzi, F.; Mosconi, E.; De Angelis, F.; Brescia, R.; Rastogi, P.; Prato, M.; Manna, L. Nearly monodisperse insulator Cs_4PbX_6 (X = Cl, Br, I) nanocrystals, their mixed halide compositions, and their transformation into $CsPbX_3$ nanocrystals. *Nano Lett.* **2017**, *17*, 1924−1930.
(25) Wu, L.; Hu, H.; Xu, Y.; Jiang, S.; Chen, M.; Zhong, Q.; Yang, D.; Liu, Q.; Zhao, Y.; Sun, B.; Zhang, Q.; Yin, Y. From nonluminescent Cs_4PbX_6 (X = Cl, Br, I) nanocrystals to highly luminescent $CsPbX_3$ nanocrystals: water-triggered transformation through a CsX-stripping mechanism. *Nano Lett.* **2017**, *17*, 5799−5804.
(26) Balakrishnan, S. K.; Kamat, P. V. Ligand assisted transformation of cubic $CsPbBr_3$ nanocrystals into two-dimensional $CsPb_2Br_5$ nanosheets. *Chem. Mater.* **2018**, *30*, 74−78.
(27) Song, J.; Li, J.; Li, X.; Xu, L.; Dong, Y.; Zeng, H. Quantum dot light-emitting diodes based on inorganic perovskite cesium lead halides ($CsPbX_3$). *Adv. Mater.* **2015**, *27*, 7162−7167.
(28) Swarnkar, A.; Chulliyil, R.; Ravi, V. K.; Irfanullah, M.; Chowdhury, A.; Nag, A. Colloidal $CsPbBr_3$ perovskite nanocrystals: luminescence beyond traditional quantum dots. *Angew. Chem., Int. Ed.* **2015**, *54*, 15424−15428.
(29) Amgar, D.; Stern, A.; Rotem, D.; Porath, D.; Etgar, L. Tunable length and optical properties of $CsPbX_3$ (X = Cl, Br, I) nanowires with a few unit cells. *Nano Lett.* **2017**, *17*, 1007−1013.
(30) Imran, M.; Di Stasio, F.; Dang, Z.; Canale, C.; Khan, A. H.; Shamsi, J.; Brescia, R.; Prato, M.; Manna, L. Colloidal synthesis of strongly fluorescent $CsPbBr_3$ nanowires with width tunable down to the quantum confinement regime. *Chem. Mater.* **2016**, *28*, 6450−6454.
(31) Kostopoulou, A.; Sygletou, M.; Brintakis, K.; Lappas, A.; Stratakis, E. Low-temperature benchtop-synthesis of all-inorganic perovskite nanowires. *Nanoscale* **2017**, *9*, 18202−18207.
(32) Zhang, D.; Eaton, S. W.; Yu, Y.; Dou, L.; Yang, P. Solution-phase synthesis of cesium lead halide perovskite nanowires. *J. Am. Chem. Soc.* **2015**, *137*, 9230−9233.
(33) Zhang, D.; Yu, Y.; Bekenstein, Y.; Wong, A. B.; Alivisatos, A. P.; Yang, P. Ultrathin colloidal cesium lead halide perovskite nanowires. *J. Am. Chem. Soc.* **2016**, *138*, 13155−13158.
(34) Liang, Z.; Zhao, S.; Xu, Z.; Qiao, B.; Song, P.; Gao, D.; Xu, X. Shape-controlled synthesis of all-inorganic $CsPbBr_3$ perovskite nanocrystals with bright blue emission. *ACS Appl. Mater. Interfaces* **2016**, *8*, 28824−28830.
(35) Sun, S.; Yuan, D.; Xu, Y.; Wang, A.; Deng, Z. Ligand-mediated synthesis of shape-controlled cesium lead halide perovskite nanocrystals via reprecipitation process at room temperature. *ACS Nano* **2016**, *10*, 3648−3657.
(36) Yang, T.; Zheng, Y.; Du, Z.; Liu, W.; Yang, Z.; Gao, F.; Wang, L.; Chou, K. C.; Hou, X.; Yang, W. Superior photodetectors based on all-inorganic perovskite $CsPbI_3$ nanorods with ultrafast response and high stability. *ACS Nano* **2018**, *12*, 1611−1617.
(37) Akkerman, Q. A.; Motti, S. G.; Srimath Kandada, A. R.; Mosconi, E.; D'Innocenzo, V.; Bertoni, G.; Marras, S.; Kamino, B. A.; Miranda, L.; De Angelis, F.; Petrozza, A.; Prato, M.; Manna, L. Solution synthesis approach to colloidal cesium lead halide perovskite nanoplatelets with monolayer-level thickness control. *J. Am. Chem. Soc.* **2016**, *138*, 1010−1016.
(38) Fu, X.; Zhang, C.; Peng, Z.; Xia, Y.; Zhang, J.; Luo, W.; Zhan, R.; Li, H.; Wang, Y.; Zhang, D. Self-assembly and photoactivation of blue luminescent $CsPbBr_3$ mesocrystals synthesized at ambient temperature. *J. Mater. Chem. C* **2018**, *6*, 1701−1708.
(39) Shamsi, J.; Rastogi, P.; Caligiuri, V.; Abdelhady, A. L.; Spirito, D.; Manna, L.; Krahne, R. Bright-emitting perovskite films by large-scale synthesis and photoinduced solid-state transformation of $CsPbBr_3$ nanoplatelets. *ACS Nano* **2017**, *11*, 10206−10213.
(40) Yang, D.; Zou, Y.; Li, P.; Liu, Q.; Wu, L.; Hu, H.; Xu, Y.; Sun, B.; Zhang, Q.; Lee, S.-T. Large-scale synthesis of ultrathin cesium lead bromide perovskite nanoplates with precisely tunable dimensions and their application in blue light-emitting diodes. *Nano Energy* **2018**, *47*, 235−242.
(41) Lv, L.; Xu, Y.; Fang, H.; Luo, W.; Xu, F.; Liu, L.; Wang, B.; Zhang, X.; Yang, D.; Hu, W.; Dong, A. Generalized colloidal synthesis of high-quality, two-dimensional cesium lead halide perovskite nanosheets and their applications in photodetectors. *Nanoscale* **2016**, *8*, 13589−13596.
(42) Shamsi, J.; Dang, Z.; Bianchini, P.; Canale, C.; Stasio, F. D.; Brescia, R.; Prato, M.; Manna, L. Colloidal synthesis of quantum confined single crystal $CsPbBr_3$ nanosheets with lateral size control up to the micrometer range. *J. Am. Chem. Soc.* **2016**, *138*, 7240−7243.
(43) Song, J.; Xu, L.; Li, J.; Xue, J.; Dong, Y.; Li, X.; Zeng, H. Monolayer and few-layer all-inorganic perovskites as a new family of two-dimensional semiconductors for printable optoelectronic devices. *Adv. Mater.* **2016**, *28*, 4861−4869.
(44) Bekenstein, Y.; Koscher, B. A.; Eaton, S. W.; Yang, P.; Alivisatos, A. P. Highly luminescent colloidal nanoplates of perovskite cesium lead halide and their oriented assemblies. *J. Am. Chem. Soc.* **2015**, *137*, 16008−16011.
(45) Akkerman, Q. A.; D'Innocenzo, V.; Accornero, S.; Scarpellini, A.; Petrozza, A.; Prato, M.; Manna, L. Tuning the optical properties of cesium lead halide perovskite nanocrystals by anion exchange reactions. *J. Am. Chem. Soc.* **2015**, *137*, 10276−10281.

DOI: 10.1021/acscentsci.8b00201
ACS Cent. Sci. 2018, 4, 668−679

(46) Guhrenz, C.; Benad, A.; Ziegler, C.; Haubold, D.; Gaponik, N.; Eychmüller, A. Solid-state anion exchange reactions for color tuning of $CsPbX_3$ perovskite nanocrystals. *Chem. Mater.* **2016**, *28*, 9033−9040.
(47) Nedelcu, G.; Protesescu, L.; Yakunin, S.; Bodnarchuk, M. I.; Grotevent, M. J.; Kovalenko, M. V. Fast anion-exchange in highly luminescent nanocrystals of cesium lead halide perovskites ($CsPbX_3$, X = Cl, Br, I). *Nano Lett.* **2015**, *15*, 5635−5640.
(48) Butkus, J.; Vashishtha, P.; Chen, K.; Gallaher, J. K.; Prasad, S. K. K.; Metin, D. Z.; Laufersky, G.; Gaston, N.; Halpert, J. E.; Hodgkiss, J. M. The evolution of quantum confinement in $CsPbBr_3$ perovskite nanocrystals. *Chem. Mater.* **2017**, *29*, 3644−3652.
(49) van der Stam, W.; Geuchies, J. J.; Altantzis, T.; van den Bos, K. H.; Meeldijk, J. D.; Van Aert, S.; Bals, S.; Vanmaekelbergh, D.; de Mello Donega, C. Highly emissive divalent-ion-doped colloidal $CsPb_{1-x}MxBr_3$ perovskite nanocrystals through cation exchange. *J. Am. Chem. Soc.* **2017**, *139*, 4087−4097.
(50) Begum, R.; Parida, M. R.; Abdelhady, A. L.; Murali, B.; Alyami, N. M.; Ahmed, G. H.; Hedhili, M. N.; Bakr, O. M.; Mohammed, O. F. Engineering interfacial charge transfer in $CsPbBr_3$ perovskite nanocrystals by heterovalent doping. *J. Am. Chem. Soc.* **2017**, *139*, 731−737.
(51) Das Adhikari, S.; Dutta, S. K.; Dutta, A.; Guria, A. K.; Pradhan, N. Chemically tailoring the dopant emission in manganese-doped $CsPbCl_3$ perovskite nanocrystals. *Angew. Chem., Int. Ed.* **2017**, *56*, 8746−8750.
(52) Huang, G.; Wang, C.; Xu, S.; Zong, S.; Lu, J.; Wang, Z.; Lu, C.; Cui, Y. Postsynthetic doping of $MnCl_2$ molecules into preformed $CsPbBr_3$ perovskite nanocrystals via a halide exchange-driven cation exchange. *Adv. Mater.* **2017**, *29*, 1700095.
(53) Koscher, B. A.; Swabeck, J. K.; Bronstein, N. D.; Alivisatos, A. P. Essentially trap-free $CsPbBr_3$ colloidal nanocrystals by postsynthetic thiocyanate surface treatment. *J. Am. Chem. Soc.* **2017**, *139*, 6566−6569.
(54) Liu, F.; Zhang, Y.; Ding, C.; Kobayashi, S.; Izuishi, T.; Nakazawa, N.; Toyoda, T.; Ohta, T.; Hayase, S.; Minemoto, T.; Yoshino, K.; Dai, S.; Shen, Q. Highly luminescent phase-stable $CsPbI_3$ perovskite quantum dots achieving near 100% absolute photoluminescence quantum yield. *ACS Nano* **2017**, *11*, 10373−10383.
(55) Swarnkar, A.; Marshall, A. R.; Sanehira, E. M.; Chernomordik, B. D.; Moore, D. T.; Christians, J. A.; Chakrabarti, T.; Luther, J. M. Quantum dot-induced phase stabilization of α-$CsPbI_3$ perovskite for high-efficiency photovoltaics. *Science* **2016**, *354*, 92−95.
(56) Sanehira, E. M.; Marshall, A. R.; Christians, J. A.; Harvey, S. P.; Ciesielski, P. N.; Wheeler, L. M.; Schulz, P.; Lin, L. Y.; Beard, M. C.; Luther, J. M. Enhanced mobility $CsPbI_3$ quantum dot arrays for record-efficiency, high-voltage photovoltaic cells. *Sci. Adv.* **2017**, *3*, eaao4204.
(57) Zhang, T.; Dar, M. I.; Li, G.; Xu, F.; Guo, N.; Grätzel, M.; Zhao, Y. Bication lead iodide 2D perovskite component to stabilize inorganic α-$CsPbI_3$ perovskite phase for high-efficiency solar cells. *Sci. Adv.* **2017**, *3*, e1700841.
(58) Kulbak, M.; Gupta, S.; Kedem, N.; Levine, I.; Bendikov, T.; Hodes, G.; Cahen, D. Cesium enhances long-term stability of lead bromide perovskite-based solar cells. *J. Phys. Chem. Lett.* **2016**, *7*, 167−172.
(59) Li, J.; Xu, L.; Wang, T.; Song, J.; Chen, J.; Xue, J.; Dong, Y.; Cai, B.; Shan, Q.; Han, B.; Zeng, H. 50-Fold EQE improvement up to 6.27% of solution-processed all-inorganic perovskite $CsPbBr_3$ QLEDs via surface ligand density control. *Adv. Mater.* **2017**, *29*, 1603885.
(60) Chiba, T.; Hoshi, K.; Pu, Y. J.; Takeda, Y.; Hayashi, Y.; Ohisa, S.; Kawata, S.; Kido, J. High-efficiency perovskite quantum-dot light-emitting devices by effective washing process and interfacial energy level alignment. *ACS Appl. Mater. Interfaces* **2017**, *9*, 18054−18060.
(61) Ramasamy, P.; Lim, D. H.; Kim, B.; Lee, S. H.; Lee, M. S.; Lee, J. S. All-inorganic cesium lead halide perovskite nanocrystals for photodetector applications. *Chem. Commun.* **2016**, *52*, 2067−2070.
(62) Li, X.; Yu, D.; Cao, F.; Gu, Y.; Wei, Y.; Wu, Y.; Song, J.; Zeng, H. Healing all-inorganic perovskite films via recyclable dissolution-recyrstallization for compact and smooth carrier channels of optoelectronic devices with high stability. *Adv. Funct. Mater.* **2016**, *26*, 5903−5912.
(63) Tang, X.; Zu, Z.; Shao, H.; Hu, W.; Zhou, M.; Deng, M.; Chen, W.; Zang, Z.; Zhu, T.; Xue, J. All-inorganic perovskite $CsPb(Br/I)_3$ nanorods for optoelectronic application. *Nanoscale* **2016**, *8*, 15158−15161.
(64) Yang, Z.; Wang, M.; Qiu, H.; Yao, X.; Lao, X.; Xu, S.; Lin, Z.; Sun, L.; Shao, J. Engineering the exciton dissociation in quantum-confined 2D $CsPbBr_3$ nanosheet films. *Adv. Funct. Mater.* **2018**, *28*, 1705908.
(65) Zhang, Q.; Su, R.; Liu, X.; Xing, J.; Sum, T. C.; Xiong, Q. High-quality whispering-gallery-mode lasing from cesium lead halide perovskite nanoplatelets. *Adv. Funct. Mater.* **2016**, *26*, 6238−6245.
(66) Zhang, Q.; Su, R.; Du, W.; Liu, X.; Zhao, L.; Ha, S. T.; Xiong, Q. Advances in small perovskite-based lasers. *Small Methods* **2017**, *1*, 1700163.
(67) Wang, Y.; Li, X.; Song, J.; Xiao, L.; Zeng, H.; Sun, H. All-inorganic colloidal perovskite quantum dots: a new class of lasing materials with favorable characteristics. *Adv. Mater.* **2015**, *27*, 7101−7108.
(68) Tan, Y.; Zou, Y.; Wu, L.; Huang, Q.; Yang, D.; Chen, M.; Ban, M.; Wu, C.; Wu, T.; Bai, S.; Song, T.; Zhang, Q.; Sun, B. Highly luminescent and stable perovskite nanocrystals with octylphosphonic acid as a ligand for efficient light-emitting diodes. *ACS Appl. Mater. Interfaces* **2018**, *10*, 3784−3792.
(69) Wu, L.; Zhong, Q.; Yang, D.; Chen, M.; Hu, H.; Pan, Q.; Liu, H.; Cao, M.; Xu, Y.; Sun, B.; Zhang, Q. Improving the stability and size tunability of cesium lead halide perovskite nanocrystals using trioctylphosphine oxide as the capping ligand. *Langmuir* **2017**, *33*, 12689−12696.
(70) Krieg, F.; Ochsenbein, S. T.; Yakunin, S.; Ten Brinck, S.; Aellen, P.; Suess, A.; Clerc, B.; Guggisberg, D.; Nazarenko, O.; Shynkarenko, Y.; Kumar, S.; Shih, C. J.; Infante, I.; Kovalenko, M. V. Colloidal $CsPbX_3$ (X = Cl, Br, I) nanocrystals 2.0: zwitterionic capping ligands for improved durability and stability. *ACS Energy Lett.* **2018**, *3*, 641−646.
(71) Pan, J.; Quan, L. N.; Zhao, Y.; Peng, W.; Murali, B.; Sarmah, S. P.; Yuan, M.; Sinatra, L.; Alyami, N. M.; Liu, J.; Yassitepe, E.; Yang, Z.; Voznyy, O.; Comin, R.; Hedhili, M. N.; Mohammed, O. F.; Lu, Z. H.; Kim, D. H.; Sargent, E. H.; Bakr, O. M. Highly efficient perovskite-quantum-dot light-emitting diodes by surface engineering. *Adv. Mater.* **2016**, *28*, 8718−8725.
(72) Pan, J.; Shang, Y.; Yin, J.; De Bastiani, M.; Peng, W.; Dursun, I.; Sinatra, L.; El-Zohry, A. M.; Hedhili, M. N.; Emwas, A. H.; Mohammed, O. F.; Ning, Z.; Bakr, O. M. Bidentate ligand-passivated $CsPbI_3$ perovskite nanocrystals for stable near-unity photoluminescence quantum yield and efficient red light-emitting diodes. *J. Am. Chem. Soc.* **2018**, *140*, 562−565.
(73) Li, X.; Wang, Y.; Sun, H.; Zeng, H. Amino-mediated anchoring perovskite quantum dots for stable and low-threshold random lasing. *Adv. Mater.* **2017**, *29*, 1701185.
(74) Pan, A.; Jurow, M. J.; Qiu, F.; Yang, J.; Ren, B.; Urban, J. J.; He, L.; Liu, Y. Nanorod suprastructures from a ternary graphene oxide-polymer-$CsPbX_3$ perovskite nanocrystal composite that display high environmental stability. *Nano Lett.* **2017**, *17*, 6759−6765.
(75) Wei, Y.; Deng, X.; Xie, Z.; Cai, X.; Liang, S.; Ma, P. a.; Hou, Z.; Cheng, Z.; Lin, J. Enhancing the stability of perovskite quantum dots by encapsulation in crosslinked polystyrene beads via a swelling-shrinking strategy toward superior water resistance. *Adv. Funct. Mater.* **2017**, *27*, 1703535.
(76) Wang, H. C.; Lin, S. Y.; Tang, A. C.; Singh, B. P.; Tong, H. C.; Chen, C. Y.; Lee, Y. C.; Tsai, T. L.; Liu, R. S. Mesoporous silica particles integrated with all-inorganic $CsPbBr_3$ perovskite quantum-dot nanocomposites (MP-PQDs) with high stability and wide color gamut used for backlight display. *Angew. Chem., Int. Ed.* **2016**, *55*, 7924−7929.
(77) Raja, S. N.; Bekenstein, Y.; Koc, M. A.; Fischer, S.; Zhang, D.; Lin, L.; Ritchie, R. O.; Yang, P.; Alivisatos, A. P. Encapsulation of perovskite nanocrystals into macroscale polymer matrices: enhanced

DOI: 10.1021/acscentsci.8b00201
ACS Cent. Sci. 2018, 4, 668−679

stability and polarization. *ACS Appl. Mater. Interfaces* **2016**, *8*, 35523−35533.
(78) Loiudice, A.; Saris, S.; Oveisi, E.; Alexander, D. T. L.; Buonsanti, R. $CsPbBr_3$ QD/AlOx inorganic nanocomposites with exceptional stability in water, light, and heat. *Angew. Chem., Int. Ed.* **2017**, *56*, 10696−10701.
(79) Huang, H.; Chen, B.; Wang, Z.; Hung, T. F.; Susha, A. S.; Zhong, H.; Rogach, A. L. Water resistant $CsPbX_3$ nanocrystals coated with polyhedral oligomeric silsesquioxane and their use as solid state luminophores in all-perovskite white light-emitting devices. *Chem. Sci.* **2016**, *7*, 5699−5703.
(80) Dirin, D. N.; Protesescu, L.; Trummer, D.; Kochetygov, I. V.; Yakunin, S.; Krumeich, F.; Stadie, N. P.; Kovalenko, M. V. Harnessing defect-tolerance at the nanoscale: highly luminescent lead halide perovskite nanocrystals in mesoporous silica matrixes. *Nano Lett.* **2016**, *16*, 5866−5874.
(81) Li, Z.; Kong, L.; Huang, S.; Li, L. Highly luminescent and ultrastable $CsPbBr_3$ perovskite quantum dots incorporated into a silica/alumina monolith. *Angew. Chem.* **2017**, *129*, 8246−8250.
(82) Hu, H.; Wu, L.; Tan, Y.; Zhong, Q.; Chen, M.; Qiu, Y.; Yang, D.; Sun, B.; Zhang, Q.; Yin, Y. Interfacial synthesis of highly stable $CsPbX_3$/oxide Janus nanoparticles. *J. Am. Chem. Soc.* **2018**, *140*, 406−412.
(83) Reiss, P.; Protiere, M.; Li, L. Core/Shell semiconductor nanocrystals. *Small* **2009**, *5*, 154−168.
(84) Jellicoe, T. C.; Richter, J. M.; Glass, H. F.; Tabachnyk, M.; Brady, R.; Dutton, S. E.; Rao, A.; Friend, R. H.; Credgington, D.; Greenham, N. C.; Bohm, M. L. Synthesis and optical properties of lead-free cesium tin halide perovskite nanocrystals. *J. Am. Chem. Soc.* **2016**, *138*, 2941−2944.
(85) Wang, A.; Yan, X.; Zhang, M.; Sun, S.; Yang, M.; Shen, W.; Pan, X.; Wang, P.; Deng, Z. Controlled synthesis of lead-free and stable perovskite derivative Cs_2SnI_6 nanocrystals via a facile hot-injection process. *Chem. Mater.* **2016**, *28*, 8132−8140.
(86) Sabba, D.; Mulmudi, H. K.; Prabhakar, R. R.; Krishnamoorthy, T.; Baikie, T.; Boix, P. P.; Mhaisalkar, S.; Mathews, N. Impact of anionic Br−substitution on open circuit voltage in lead free perovskite ($CsSnI_{3-x}Br_x$) solar cells. *J. Phys. Chem. C* **2015**, *119*, 1763−1767.
(87) Chung, I.; Song, J. H.; Im, J.; Androulakis, J.; Malliakas, C. D.; Li, H.; Freeman, A. J.; Kenney, J. T.; Kanatzidis, M. G. $CsSnI_3$: Semiconductor or metal? High electrical conductivity and strong near-infrared photoluminescence from a single material. High hole mobility and phase-transitions. *J. Am. Chem. Soc.* **2012**, *134*, 8579−8587.
(88) Yang, B.; Chen, J.; Hong, F.; Mao, X.; Zheng, K.; Yang, S.; Li, Y.; Pullerits, T.; Deng, W.; Han, K. Lead-free, air-stable all-inorganic cesium bismuth halide perovskite nanocrystals. *Angew. Chem., Int. Ed.* **2017**, *56*, 12471−12475.
(89) Lou, Y.; Fang, M.; Chen, J.; Zhao, Y. Formation of highly luminescent cesium bismuth halide perovskite quantum dots tuned by anion exchange. *Chem. Commun.* **2018**, *54*, 3779−3782.
(90) Zhang, Y.; Yin, J.; Parida, M. R.; Ahmed, G. H.; Pan, J.; Bakr, O. M.; Bredas, J. L.; Mohammed, O. F. Direct-indirect nature of the bandgap in lead-free perovskite nanocrystals. *J. Phys. Chem. Lett.* **2017**, *8*, 3173−3177.
(91) Zhang, J.; Yang, Y.; Deng, H.; Farooq, U.; Yang, X.; Khan, J.; Tang, J.; Song, H. High quantum yield blue emission from lead-free inorganic antimony halide perovskite colloidal quantum dots. *ACS Nano* **2017**, *11*, 9294−9302.
(92) Zhou, L.; Xu, Y.-F.; Chen, B.-X.; Kuang, D.-B.; Su, C.-Y. Synthesis and photocatalytic application of Stable lead-free $Cs_2AgBiBr_6$ perovskite nanocrystals. *Small* **2018**, *14*, 1703762.
(93) Creutz, S. E.; Crites, E. N.; De Siena, M. C.; Gamelin, D. R. Colloidal nanocrystals of lead-free double-perovskite (elpasolite) semiconductors: synthesis and anion exchange to access new materials. *Nano Lett.* **2018**, *18*, 1118−1123.
(94) Volonakis, G.; Haghighirad, A. A.; Milot, R. L.; Sio, W. H.; Filip, M. R.; Wenger, B.; Johnston, M. B.; Herz, L. M.; Snaith, H. J.; Giustino, F. $Cs_2InAgCl_6$: A new lead-free halide double perovskite with direct band gap. *J. Phys. Chem. Lett.* **2017**, *8*, 772−778.
(95) Zhao, X.-G.; Yang, J.-H.; Fu, Y.; Yang, D.; Xu, Q.; Yu, L.; Wei, S.-H.; Zhang, L. Design of Lead-Free Inorganic Halide Perovskites for Solar Cells via Cation-Transmutation. *J. Am. Chem. Soc.* **2017**, *139*, 2630−2638.
(96) Xu, Y. F.; Yang, M. Z.; Chen, B. X.; Wang, X. D.; Chen, H. Y.; Kuang, D. B.; Su, C. Y. A $CsPbBr_3$ perovskite quantum dot/graphene oxide composite for photocatalytic CO_2 reduction. *J. Am. Chem. Soc.* **2017**, *139*, 5660−5663.

DOI: 10.1021/acscentsci.8b00201
ACS Cent. Sci. 2018, 4, 668−679